Quantum Electronics **48** (10) 894–897 (2018)

https://doi.org/10.1070/QEL16762

Quantum memory in the revival of silenced echo scheme in an optical resonator

M.M. Minnegaliev, K.I. Gerasimov, R.V. Urmancheev, S.A. Moiseev

Abstract. **The protocol of optical quantum memory in the revival of silenced photon echo (ROSE) scheme is experimentally implemented in a $Tm^{3+}:Y_3Al_5O_{12}$ crystal (c = 0.1 at.%) placed in an impedance-matched optical Fabry–Perot resonator. The input signal recovery efficiency of ~21% is achieved for a light pulse with a storage time of 36 μs. The main sources of loss and their impact on the achieved quantum efficiency are discussed, as well as the advantages of the implemented scheme and the possibilities of the further improvement of the main parameters of quantum memory.**

Keywords: *quantum memory, photon echo, optical resonator, crystals with rare earth ions, ROSE protocol.*

Rapid progress in optical quantum technologies, including optical quantum computations [1, 2] and long-distance quantum communications [3, 4], stimulates the development of quantum memory (QM) [5–7]. The implementation of high-efficiency QM will not only considerably extend the capabilities of these technologies, but will also open new lines of research and practical engineering. During the last decade, a number of efficient QM protocols for writing and reading optical signals has been proposed and experimentally implemented [8, 9] basing on the electromagnetically induced transparency (EIT) [10–12], the photon echo with controlled reversible inhomogeneous broadening (CRIB) [13, 14], and its version with an external control gradient magnetic/electric (GEM) field [8, 9, 15], as well as the QM based on the atomic frequency comb (AFC) [16–20] and on nonresonance Raman interaction [21, 22], including that in combination with photon echo [23] and in the scheme of fast quantum memory [24].

For most protocols, the possibility to achieve high efficiency [8, 9], multimode capacity [25, 26], broadband operation [27] and high accuracy of retrieval of input quantum states [28] have been shown theoretically and experimentally. The schemes of QM based on the photon echo effect in solid-state systems [6] have demonstrated the best capabilities for saving multipulse light fields with high quantum efficiency. In turn, the advantages of the QM scheme with revival of silenced echo (ROSE) [29, 30] consist in the simplicity of experimental implementation, the possibility to work with single-photon fields [31], as well as the addressable reading of recorded qubits [32].

M.M. Minnegaliev, K.I. Gerasimov, R.V. Urmancheev, S.A. Moiseev
Kazan Quantum Center, A.N. Tupolev Kazan National Research Technical University, ul. K. Marksa 10, 420111 Kazan, Russia;
e-mail: s.a.moiseev@kazanqc.org

Received 11 June 2018; revision received 19 July 2018
Kvantovaya Elektronika **48** (10) 894–897 (2018)
Translated by V.L. Derbov

Note that in this protocol the use of control laser fields offers a possibility to control the write/read processes, as well as additional manipulations with quantum states of signal fields. In multiple experimental studies of the photon echo QM, the crystals doped with rare-earth ions (REI) are the most popular media for using as a memory cell [33, 34]. The presence of long-lived electron-nuclear spin states in these ions makes it possible to increase the QM lifetime up to $\sim 10^3$ s [35], and the large inhomogeneous linewidth of optical transitions allows broadband QM to be implemented in such crystals [26].

It is worth noting that the enhancement of controlled interaction of single photons with matter remains to be one of important problems in the development of high-efficiency QM. In Ref. [30], we experimentally implemented the ROSE protocol of QM using the orthogonal propagation geometry of signal and control light beams. With the optimal optical density of the sample and the ideal parameters of rephasing laser pulse, the maximal efficiency of QM does not exceed 54% in the case of copropagating signal and recalled light fields. In an impedance-matched optical resonator [36, 37] one can implement the required degree of light–matter interaction providing complete absorption of the input optical signals with the achievement of extremely high (close to 100%) QM efficiency. In turn, the enhancement of coupling between photons and matter allows one to use crystals with a lower REI concentration, which inhibits unwanted interactions between the particles and increases the lifetime of coherence, excited in the system of ions. The described advantages were partially implemented in recent papers [38–41] for the AFC protocol in an optical resonator.

The goal of the present paper is to implement experimentally the ROSE protocol in an optical resonator. As in our previous paper [30], we use the orthogonal geometry of propagation of the signal and control laser fields (Fig. 1). The role of a QM cell is played by a $Tm^{3+}:Y_3Al_5O_{12}$ crystal (c = 0.1 at.%) having the shape of a parallelepiped measuring 2×3×8 mm and the edges parallel to the crystallographic axes [110], [001], and [$\bar{1}$10]. The crystal was placed in a closed-cycle cryostat (Montana Instruments Corp.), where it was cooled down to 4.0 ± 0.1 K. Under such conditions, the inhomogeneous broadening of the optical transition amounted to ~20 GHz, and the absorption αL in the line centre attained 1.75 cm^{-1} (α being the absorption coefficient of the crystal and L being its length). The phase memory time T_M [42] was found from the experiments on the decay of a two-pulse photon echo signal, which amounted to 55 μs for x = 1.8 ($I_e = I_0 \exp[-2(2\tau/T_M)^x]$, where τ is the time delay between two pulses). The signal and control laser beams propagate along the axes [001] and [$\bar{1}$10], respectively, and their polarisations are parallel to the [110] crystal axis. A continuous-wave

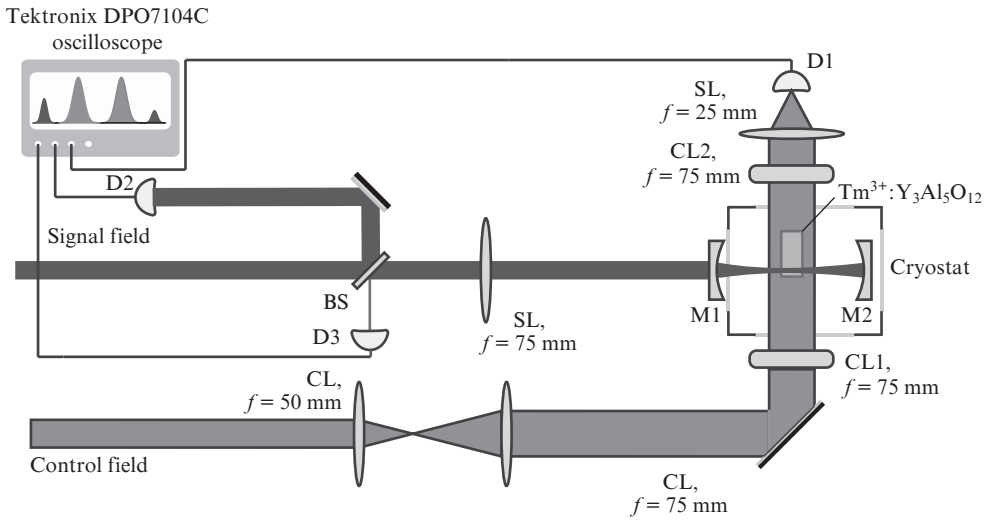

Figure 1. Simplified of the experimental setup: (M1 and M2) front and back mirrors of the concentric resonator with reflection coefficients R_1 and R_2, respectively; (CL1, CL2) cylindrical lenses; (SL) spherical lenses; (BS) 50 : 50 beam splitter; (D1) photodetector; (D2, D3) Thorlabs APD120A/M photodetectors.

Tekhnoscan TIS-SF-777 Ti : sapphire laser tuned to the optical transition $^3H_6 - {}^3H_4$ of Tm^{3+} with the wavelength λ = 793 nm is used as a radiation source. In the experiment, the pulse area of the input signal was much smaller than $\pi/2$, and one pulse contained $\sim 10^8$ photons. As in Ref. [30], we used the laser pulses with the specified amplitude and frequency modulation as control (rephasing) fields.

The concentric optical cavity is formed by two spherical dielectric mirrors having the reflection coefficients $R_1 = 70\%$ for the front mirror and $R_2 \approx 99.9\%$ for the back one. The total length of the resonator is ~90 mm, which corresponded to the free spectral range of 1.65 GHz. The impedance-matching condition for coupling the resonator with the incident signal radiation is achieved when the sum of all three kinds of internal losses inside the resonator (the losses at optical elements and the absorption in the crystal) is equal to the transmission coefficient of the front mirror $T_1 = 1 - R_1$. In this case, the reflection of the input signal from the front mirror is absent and all power of radiation incident on the first mirror is transmitted and absorbed in the resonator. If the parasitic losses at the mirrors are neglected, then the main losses will be determined by the absorption of light in the crystal. For complete absorption of input light, the impedance-matching condition is $2\alpha L = -\ln R_1$. In our case this condition is satisfied for $\alpha L \approx 0.15$. Figure 2 presents the experimental dependences of the reflection of the resonator signal pulse on the laser radiation frequency, varied within the inhomogeneously broadened absorption line of the crystal. The best matching of the cavity coupling is achieved at the frequency 377.879 GHz, i.e., at the edge of the absorption line of thulium ions (grey curve in Fig. 2).

The finesse F of an ideally aligned resonator with the reflection coefficients R_1 and R_2 without the internal losses taken into account should be equal to 17.5. However, during the experiment additional losses took place inside the resonator, which were produced by one of the two optical windows of the cryostat vacuum chamber (with the reflection coefficient less than 0.5%) and two AR-coated faces of the crystal (with the reflection coefficient of each face ~1%). Under such conditions, the experimentally measured finesse of the resonator is F = 14.5 beyond the limits of the crystal absorption line, which agrees with the theoretical estimate $F = \pi \exp(-\alpha L/2)/$

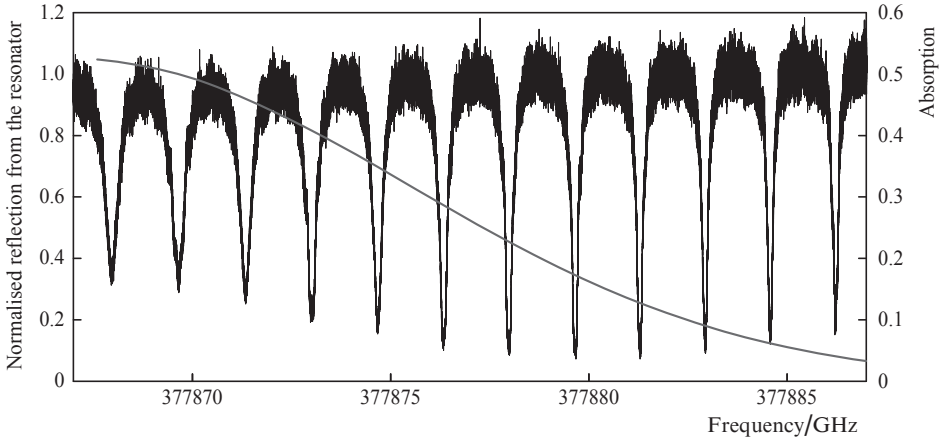

Figure 2. Normalised reflection peaks of the Fabry–Perot resonator (black curve) and absorption αL of thulium ions (grey curve) in the Tm^{3+}:$Y_3Al_5O_{12}$ crystal (c =0.1 at.%) vs. the radiation frequency.

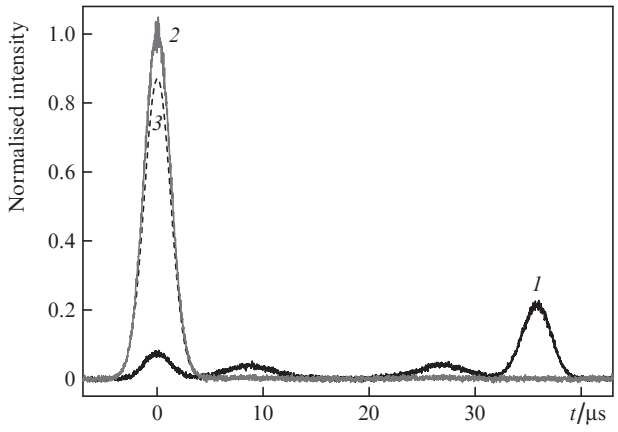

Figure 3. (*1*) Silenced echo signal (at t = 36 μs), (*2*) input pulse (at t = 0), and its unabsorbed reflected part, as well as signals from the scattered control π-pulses [between t = 0 and t = 36 μs, curve (*1*)]; (*3*) unabsorbed fraction of the input pulse for a single-pass scheme without the optical resonator.

$[1 - \exp(-\alpha L)]$, where $\alpha = \alpha_{Tm} - \ln(R_1R_2\alpha_0)/(2L)$, α_{Tm} is the optical density of the crystal of length L, and $(1-\alpha_0)\times 100\% = 5\%$ are the parasitic losses inside the resonator.

Figure 3 presents the result of revival of a silenced echo signal in the optical resonator in the impedance-matched coupling regime. The efficiency of the signal pulse recovery amounted to ~21% for the storage time 36 μs. The capacity of the studied QM in the experiment appeared to be 9 (the spectral width of the input pulse 250 kHz multiplied by the storage time 36 μs). Note that for the inhomogeneous broadening of the optical transition line equal to 20 GHz one can use the signal and control π-pulses with a broader band, which will allow the QM cell capacity to be increased by orders of magnitude even at moderate increase in the signal storage time.

As seen from Fig. 3, the complete impedance-matching condition of the resonator coupling was not achieved in the experiment, since ~7.5% of the input pulse energy is reflected from the input mirror of the resonator. We explain this mismatch by the nonideal alignment of the resonator mirrors and partly by poor spatial mode matching. Nevertheless, the use of the optical resonator allowed the input signal absorption to be increased in the crystal by more than 10 times. In the single-pass memory scheme at the same frequency the crystal absorbs only 12.5% of the input pulse energy [curve (*3*) in Fig. 3]. The deviation from the exact impedance-matching condition leads to a reduction of quantum efficiency of the signal pulse recovery. However, the main reason of the efficiency reduction in the performed experiment were the effects of decoherence at the optical transition of thulium ions.

As mentioned above, the time of phase memory T_M that determines the upper limit of the acceptable delay time in the QM cell amounts to 55 μs (x = 1.8). This leads to a fall of quantum efficiency from 100% to 40% according to the dependence $\exp[-2(2\tau/T_M)^x]$ (2τ being the full time of the signal storage in the memory cell). Nevertheless, this time can be increased in a few ways. First, as already mentioned above, due to the presence of an optical resonator that provides enhanced light–matter interaction, one can use crystals with a smaller REI concentration that possess longer time of phase memory. Second, in Ref. [43] it was shown that when the Tm^{3+}:YAG crystal is placed in a weak external magnetic field, the time T_M can be increased by a few times. Third, the most promising way of increasing the phase memory time is the transfer of optical coherence to the electron–nuclear sublevels. As known, in some crystals the coherence time T_2 between hyperfine sublevels in the ground state of REI can attain 1.3 s [44]. By using dynamic decoupling methods at so-called clock transitions between hyperfine sublevels, e.g., in the $^{151}Eu^{3+}:Y_2SiO_5$ crystal, the coherence time can be increased by orders of magnitude and become as large as 6 hours [35].

Thus, in the present paper the revival of silenced echo QM protocol in the $Tm^{3+}:Y_3Al_5O_{12}$ (c = 0.1 at.%) crystal placed in an impedance-matched optical resonator is experimentally implemented for the first time. The quantum efficiency 21% of storing a single light pulse in the crystal during 36 μs is achieved. As shown by the analysis of experimental data, it is possible to increase the quantum efficiency significantly in the studied QM protocol with our crystal, if one would use shorter light pulses and shorter storage times, as well as by using crystals with longer coherence times of quantum transitions. It is remarkable that the implemented QM protocol allows efficient and rather simple exploitation of natural inhomogeneous broadening of quantum systems, which makes its further development promising.

Further studies will be devoted to the implementation of this protocol in other crystals and optical resonators, including those integrated in optical fibre circuits [41, 45, 46], where the achievement of the basic parameters of QM remains one of the primary tasks.

Acknowledgements. This work was supported by the Russian Science Foundation (Grant No. 14-12-01333 P).

References

1. Knill E., Laflamme R., Milburn G.J. *Nature*, **409**, 46 (2001).
2. Kok P. et al. *Rev. Mod. Phys.*, **79**, 135 (2007).
3. Cirac J.I., Zoller P. *Phys. Rev. Lett.*, **81**, 5932 (1998).
4. Sangouard N., Simon C., De Riedmatten H., Gisin N. *Rev. Mod. Phys.*, **83**, 33 (2011).
5. Lvovsky A.I., Sanders B.C., Tittel W. *Nat. Photon.*, **3**, 706 (2009).
6. Tittel W. et al. *Laser Photon. Rev.*, **4**, 244 (2009).
7. Heshami K. et al. *J. Mod. Opt.*, **63**, 2005 (2016).
8. Hosseini M., Sparkes B.M., Campbell G., Lam P.K., Buchler B.C. *Nat. Commun.*, **2**, 174 (2011).
9. Hedges M.P., Longdell J.J., Li Y., Sellars M.J. *Nature*, **465**, 1052 (2010).
10. Schraft D., Hain M., Lorenz N., Halfmann T. *Phys. Rev. Lett.*, **116**, 073602 (2016).
11. Heinze G., Hubrich C., Halfmann T. *Phys. Rev. Lett.*, **111**, 033601 (2013).
12. Phillips N.B., Gorshkov A.V., Novikova I. *Phys. Rev. A*, **78**, 023801 (2008).
13. Moiseev S.A., Kröll S. *Phys. Rev. Lett.*, **87**, 173601 (2001).
14. Kraus B. et al. *Phys. Rev. A*, **73**, 020302 (2006).
15. Hétet G., Longdell J.J., Sellars M.J., Lam P.K., Buchler B.C. *Phys. Rev. Lett.*, **101**, 203601 (2008).
16. Akhmedzhanov R.A. et al. *Laser Phys. Lett.*, **13**, 015202 (2016).
17. Sabooni M. et al. *Phys. Rev. Lett.*, **105**, 060501 (2010).
18. Amari A. et al. *J. Lumin.*, **130**, 1579 (2010).
19. Zhou Z.Q., Lin W.B.,Yang M., Li C.F., Guo G.C. *Phys. Rev. Lett.*, **108**, 190505 (2012).
20. Zhou Z.Q., Wang J., Li C.F., Guo G.C. *Sci. Rep.*, **3**, 2754 (2013).
21. Zhang X., Kalachev A., Kocharovskaya O. *Phys. Rev. A*, **90**, 052322 (2014).
22. Reim K.F. et al. *Nat. Photon.*, **4**, 218 (2010).
23. Moiseev S.A. *Phys. Rev. A*, **88**, 012304 (2013).
24. Tikhonov K., Samburskaya K., Golubeva T., Golubev Y. *Phys. Rev. A*, **89**, 013811 (2014).

25. Afzelius M., Simon C., De Riedmatten H., Gisin N. *Phys. Rev. A*, **79**, 052329 (2009).
26. Bonarota M., Le Gouët J.L., Chanelière T. *New J. Phys*., **13**, 013013 (2011).
27. Saglamyurek E. et al. *Nature*, **469**, 512 (2011).
28. Hsiao Y.-F. et al. *Phys. Rev. Lett*., **120**, 183602 (2018).
29. Damon V., Bonarota M., Louchet-Chauvet A., Chanelière T., Le Gouët J.L. *New J. Phys*., **13**, 093031 (2011).
30. Gerasimov K.I. et al. *Opt. Spectrosc*., **123**, 200 (2017).
31. Bonarota M., Dajczgewand J., Louchet-Chauvet A., Le Gouët J.-L., Chanelière T. *Laser Phys*., **24**, 094003 (2014).
32. Gerasimov K., Minnegaliev M., Urmancheev R., Moiseev S. *EPJ Web Conf*., **161**, 01012 (2017).
33. Thiel C.W., Böttger T., Cone R.L. *J. Lumin*., **131**, 353 (2011).
34. Macfarlane R.M. *J. Lumin*., **100**, 1 (2003).
35. Zhong M. et al. *Nature*, **517**, 177 (2015).
36. Afzelius M., Simon C. *Phys. Rev. A*, **82**, 022310 (2010).
37. Moiseev S.A., Andrianov S.N., Gubaidullin F.F. *Phys. Rev. A*, **82**, 022311 (2010).
38. Sabooni M., Li Q., Kröll S., Rippe L. *Phys. Rev. Lett*., **110**, 133604 (2013).
39. Jobez P. et al. *New J. Phys*., **16**, 083005 (2014).
40. Akhmedzhanov R.A. et al. *Laser Phys. Lett*., **13**, 115203 (2016).
41. Zhong T. et al. *Science*, **357**, 1392 (2017).
42. Mims W.B. *Phys. Rev*., **168**, 370 (1968).
43. Thiel C.W. et al. *Laser Phys*., **24** (10), 106002 (2014).
44. Rančić M. et.al. *Nat. Phys*., **14** (1), 50 (2017).
45. Minnegaliev M.M. et al. *Laser Phys. Lett*., **15**, 045207 (2018).
46. Corrielli G., Seri A., Mazzera M., Osellame R., De Riedmatten H. *Phys. Rev. Appl*., **5**, 054013 (2016).